

# Chapter 1

## Developing Vapor Intrusion Models

### 1.1 Introduction

No models are true representations of reality, but some of them may be useful. Ever since Newton first wrote his laws of motion, mankind has tried to describe reality with an ever increasing number of mathematical statements. With the advent of computation and advancements in numerical methods our capabilities to mathematically describe physical systems has dramatically increased. Even so, real-world systems are too complex to be fully modeled, but mathematical representations may be used to approximate and reveal useful insights of how they function.

This is especially true for vapor intrusion (VI) models. Often it is impossible or difficult to conduct controlled studies of VI sites making models an important tool for understanding these sites and the VI phenomena. The previous chapter is proof of this as it is readily apparent that a multitude of VI models of varying complexity have been developed over the years, and has become an important part of the scientific VI community. From the simple Johnson & Ettinger one-dimensional model to full three-dimensional finite element models (FEM) we see that the increased complexity of the model allowed for a greater number of VI topics and phenomena to be explored.

The processes of VI may be described by partial differential equations (PDEs). Unfortunately, there rarely are any analytical solutions to these (except in the most simple cases) and numerical methods are required to find approximate solutions. One of the most powerful numerical methods for solving PDEs is the finite element method, which not only allows us to find solutions to PDEs but does so for complex three-dimensional geometries.

The purposes of this thesis is not to explain the FEM in any great detail, but there are many great resources available for those who are interested to learn more. There are however, two things that are important to know what makes the FEM unique.

The first is the FEM divides up a complicated geometry into smaller *finite elements*, hence its name. Which elements exactly depend on the dimensionality of the model and the specific problem that one wish to solve. Three-dimensional geometries are usually represented by tetrahedral and two-dimensional ones by triangles.

The second is that the solution to a PDE may be represented by a linear com-

Figure 1.1: Example of a simple conceptual site model of a vapor intrusion site.

bination of a series of *basis functions* with an associated function *coefficient*.

$$u \approx \sum_i u_i \psi_i \quad (1.1)$$

where  $u$  is the solution to the PDE,  $u_i$  is the coefficient associated with the basis function  $\psi_i$ . This approximation allows the PDE to be discretized into a matrix and the  $u_i$  coefficients are solved for. Any function may serve as a *basis function*, but typically a simple one is chosen (for simpler computation) like a linear hat function or low-degree polynomial. In certain applications, some basis functions perform better than other, but in most cases linear hat functions or second-degree polynomials are preferable.

The development of the three-dimensional finite element vapor intrusion models begin with a conceptual site model (CSM) of a VI site. In general when one develops models, it is best in the beginning to keep the model as simple as possible, and not to add overly complex features or excessive physics. As such, we begin with a very simple CSM which may be seen in Figure 1.1.

This CSM features a residential building with a 10 by 10 m footprint, with a concrete foundation one meter below ground-surface (bgs). Along the perimeter of foundation there is a one cm wide breach, through the subsurface contaminants enter the house. Three meters below the foundation, there is a contaminated groundwater source, from which contaminants vapor continuously evaporate. The house is assumed to be depressurized relative to the atmosphere which creates a pressure gradient, allowing air to be pulled through the ground-surface, soil, and into the house - carrying some contaminants with it. The indoor air is also exchanged at a constant rate with the outside environment, which is the only way the contaminant leave the house. For simplicity we also assume that the soil is completely homogenous.

To implement this CSM as a finite-element model several steps must be followed.

1. Construct a model geometry (domain).
2. Assign relevant partial differential equations (PDEs) and boundary conditions (BCs) that describe the physics.
3. Mesh the geometry.
4. Configure and choose solvers.
5. Post-processing.

Each step will be carefully explained, beginning with the construction of the domain.

## 1.2 Geometry

Designing the model geometry is the first step to creating a 3D FEM model. It is one of the most important steps, as the geometry will dictate the model accuracy and astute geometry design will help save computational resources. When designing a geometry the FEM user should have the following goals in mind:

1. Represent the model geometry as accurately as possible.
2. Avoid unnecessarily fine details.
3. Try to leverage symmetry to reduce geometry size.

The first point is somewhat self-explanatory, as we obviously want to create a model geometry that is as similar to what we want to model as possible. The second points can at times run counter to the first and may be more self-evident once meshing is more thoroughly discussed. Tiny details often require a significant number of mesh elements to be fully resolved, disproportionally adding to the total number of mesh element, and may significantly increase computational costs. This is when the skill and judgement of the modeler comes in - choosing which details to omit and which to keep. As a rule-of-thumb one should for the most part try to only model parts of the geometry that is of significant value to the question that one wants answered. In VI modeling, one such obvious area is the crack or breach in the foundation through which contaminant vapors enter the structure, resolving this tiny part of the geometry is of great importance.

The third point is something that the modeler should always be on the lookout for when designing a model geometry - if there are any planes of symmetry in the geometry. Finding a plane of symmetry allows us to reduce the size of the model and save significantly computational costs. A simple example of this is one wants to model a pipe with static mixers inside, then only a sector of the cylinder's face may be necessary to be modeled. Using the simple CSM described by Figure 1.1 only a quarter of the house and surrounding property is necessary to be explicitly modeled, cutting the number of required mesh elements down to just a quarter of what would otherwise be necessary - a huge computational saving!

### 1.2.1 Geometric Components

Model geometries are typically designed in some sort of computer assisted design (CAD) software. The exact tools and techniques available to the modeler will vary from software to software, with some featuring import options for real-world scanned 3D geometries to combining simple geometric objects through various Boolean operations. The software we use, COMSOL, uses primarily the latter method of combining simple objects to form more complicated ones but more capabilities may be purchased.

To create a model geometry of the CSM in Figure 1.1, only a few simple geometric objects and Boolean operations are required - two cuboids, two rectangles, one Boolean difference operation, and one Boolean join operation. The following steps are needed:

1. Create a block or cuboid that is 15 meter wide and long, and with a height of 4 meter.
2. Create another block that is 5 meter wide and long, with a height of 1 meter.
3. Place the second block 3 meter above zero, so that the top surfaces of the two blocks intersect.
4. Perform a difference operation, removing the smaller block from the first one.

At this point you will see that a quarter soil domain has been created, with an empty space that will represent a house with a foundation slab located 1 meter below ground-surface.

The attentive reader will now of course notice that an entire house is missing from the model geometry. This is intentional, as explicitly modeling the interior of a building is too impractical for two primarily two reasons. First is that house interiors are simply too diverse for any explicit model to truly be representative in any general sense, not to mention how laborious it would be to create such a model interior. Secondly, the computational costs required to solve the air flow inside (necessary for accurate representation of contaminant transport/distribution inside) would be significant. The Navier-Stokes equation would need to be solved, and even using one of the simpler versions of it (large eddy simulation or Reynold's averaged) would impose a significant cost at questionable gain. Therefore the indoor air is modeled implicitly, which will be covered in detailed in section 1.3.

The foundation crack will be modeled as a 1 centimeter wide strip that spans the perimeter of the surface that represents the house foundation. To create the crack do the following:

1. Create a work plane 3 meter above zero.
2. Create two rectangles that are as long as the foundation, with a width of 1 centimeter, rotating one 90 degrees, and making sure that they are place along the foundation perimeter.
3. Join the two rectangles using a Boolean union (do not keep the interior boundaries).

Now that the foundation crack is generated, we have designed a model geometry of the simple CSM and the complete geometry may be seen in Figure 1.2. The next step is to choose and setup the appropriate physics required to model VI, beginning with modeling the indoor environment.

Figure 1.2: The complete geometry of the CSM described in Figure 1.1.

In the appendix, there will be further explanations for additions to the model geometry that will be necessary for modeling various VI scenarios.

## 1.3 The Indoor Environment

The indoor air space is perhaps the most important part of modeling VI, as the goal of these models ultimately is to predict indoor exposure given external factors. One could therefore assume that most of the effort in modeling VI should be spent to accurately represent the interior. This would be very impractical however, as building interiors are so diverse. Even if one would spend the time to model an interior, this would dramatically increase the number of mesh elements required to solve the model. Additionally, the air flow inside the building must be calculated, and even using a simplified version of Navier-Stokes, like large eddy simulation or Reynolds averaged, the computational cost would be significant.

To overcome this, the indoor environment is instead modeled as a continuously stirred tank reactor (CSTR). The fundamental assumption of a CSTR is that any contaminant or chemical species entering, or inside the indoor air space (control volume), is perfectly mixed, i.e. there are no spatial gradients, and is given by the ordinary differential equation (ODE) (1.2).

$$V \frac{\partial c_{\text{in}}}{\partial t} = n - V A_e c + R \quad (1.2)$$

Here  $c_{\text{in}}$  is the indoor air contaminant concentration in  $\text{mol}/\text{m}^3$ ;  $n$  is the contaminant entry rate into the building in  $\text{mol}/\text{s}$ ;  $A_e$  is the air exchange rate, which determines the which portion of the indoor air is exchanged for a given time period, e.g. if  $A_e$  is 0.5 per hour, half of the indoor air is exchanged over one hour;  $R$  can be used to simulate sorption of contaminants vapor in the indoor environment, and if this is not of interest it can simply be set to zero; Finally,  $V$  is the volume of the building interior in  $\text{m}^3$ . Typically this is set to only reflect the volume of the floor or rooms on top of the building foundation. Since the indoor environment is does not explicitly "belong" anywhere in the COMSOL model, it is modeled using the "Global ODE" interface.

### 1.3.1 Contaminant Entry

The most important component of (1.2) is of course determining the contaminant entry rate  $n$ , and is the most challenging portion of the modeling effort. The contaminant entry rate has two transport components, advective and diffusive which depends on three factors:

1. The velocity of the contaminant vapors entering or exiting the structure though the foundation crack.
2. The contaminant vapor concentration in the near vicinity of the foundation crack.
3. The indoor air contaminant concentration itself.

**Advective Transport** The advective transport due to the bulk motion of the contaminant vapors and the flux is given by (1.3).

$$j_{\text{adv}} = \vec{u}c \quad (1.3)$$

The bulk motion of the contaminant vapor is given by the vector quantity  $\vec{u}$  in  $\text{m}/\text{s}$  and  $c$  is the contaminant vapor concentration.

**Diffusive Transport** The diffusive transport is due to a concentration gradient, modified by a diffusion coefficient, and is given by Fick's law (1.4)

$$j_{\text{diff}} = \nabla \cdot (D \nabla c) \quad (1.4)$$

Where  $\nabla$  is the del operator and  $D$  is the diffusion coefficient in  $\text{m}^2/\text{s}$ . In this formulation,  $D$  does not have to be a constant and can depend on the coordinate or concentration.

The implication of this is that (1.2) has to be coupled with the equations that describe the contaminant concentration in the soil as their solutions are dependent on each other. How this is achieved will be covered in section 1.4.3 when discussing boundary conditions.

### 1.3.2 Air Exchange Rate

The air exchange rate,  $A_e$  is the parameter that determines the rate at which the contaminant vapors leave the indoor environment. Air infiltrate and exfiltrate through a building primarily via two mechanisms

1. Through breaches and orifices in the building envelope, e.g. windows, slits, or other small opening.
2. Passive or active ventilation.

With the exception of active ventilation, where air is mechanically forced to enter or exit the building, the driving force for the in-/exfiltration is driven by a pressure gradient between the indoor and outdoor environment,  $p_{in/out}$ . These pressure gradient are primarily due to differences in indoor and outdoor temperatures and to wind striking the building and quantifying these pressures differences is covered in section 1.3.3.

**Quantifying Air Exchange Rate** While air exchange rate is largely driven by the indoor and outdoor pressure difference, it is not possible to quantify their relationship for the range of pressures that a building is naturally pressurized; there is too much uncertainty. In Figure 1.3 a two-dimensional kernel density estimation (a way to estimate probability distributions[?]) of indoor/outdoor pressure and air exchange rate from the well-studied ASU house shows the relationship between these[?]. The a darker color signifies are closer association or overlap but by the lack of any visual trends (it is all a blob) combined with a Pearson's r value of x, it is apparent that there is no real correlation between them exist.

**Building Leakage Curves** It is possible to quantify air exchange rate if a building is sufficiently pressurized through building leakage curves.

### 1.3.3 Quantifying Pressure Difference Induction

**Wind Effects** As the wind strikes a surface its velocity falls to zero, and the change in momentum is directly proportional to the change in pressure:

$$\Delta P = \frac{1}{2} \rho_{air} u_{wind}^2 \quad (1.5)$$

where  $\Delta P$  is the change in pressure;  $\rho_{air}$  is the air density; and  $u_{wind}$  is the wind speed.

In reality however, the pressure drop is not quite so straightforward due to several factors, e.g. building envelope contains various structures and may be shielded by

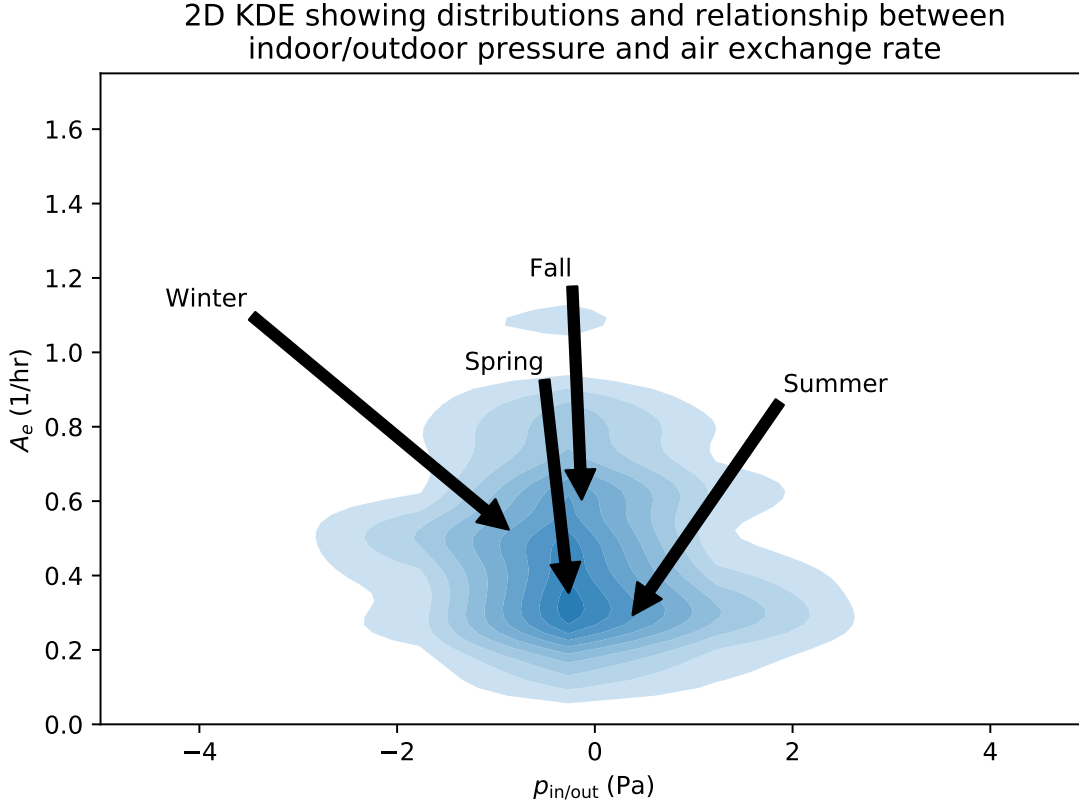


Figure 1.3: Distributions of indoor pressurization and air exchange rate and their relationships; seasonal medians indicated by arrows.

other objects. To account for this, a drag or pressure coefficient  $C_d$  is introduced to moderate the pressure drop:

$$\Delta P = C_d \frac{1}{2} \rho_{\text{air}} u_{\text{wind}}^2 \quad (1.6)$$

This coefficient is usually determined empirically from e.g. wind tunnel studies.

**Temperature Effects** The pressure of any fluid under the influence of gravity varies with elevation and the density of the fluid determines the magnitude of this pressure. Air is a compressible fluid and its density depends on its temperature. Therefore, if you separate two air masses between a wall, with each at a different temperature, a pressure difference across the wall will be induced, i.e. the *stack effect*.

Assuming the ideal gas law applies and that the temperature on either side is constant then

$$P = P_0 \exp\left(\frac{-M_{\text{air}} g z}{RT}\right) \quad (1.7)$$

determines the pressure variation across the wall. Where  $P$  is the pressure;  $P_0$  the reference pressure ( $z = 0$ );  $M_{\text{air}}$  is the molar weight of air;  $z$  is the elevation;  $g$  is the acceleration due to gravity;  $R$  is the gas constant; and  $T$  is the temperature.

This can be further simplified by defining  $z_0$  which is the height at which the pressure on both sides of the wall are equal, i.e.  $P_0$ . The pressure variation on either side can now be expressed in terms of distance from  $z_0$ ,  $z - z_0$ . Assuming

that the interior and exterior has a constant temperature of  $T_i$  and  $T_o$  respectively, the difference in pressure between the two sides along the wall is

$$\Delta P = P_0 \left[ \exp \left( \frac{-M_{\text{air}} g (z - z_0)}{RT_i} \right) - \exp \left( \frac{-M_{\text{air}} g (z - z_0)}{RT_o} \right) \right] \quad (1.8)$$

Using that  $e^{-x} = 1 - x$  for  $x \ll 1$  the pressure difference can be expressed as

$$\Delta P = \alpha \left( \frac{1}{T_o} - \frac{1}{T_i} (z - z_0) \right) \quad (1.9)$$

where  $\alpha = \frac{P_0 M_{\text{air}} g}{R} \approx 3454 \frac{\text{Pa} \cdot \text{K}}{\text{m}} \text{Pa}$ . Here a negative pressure difference,  $\Delta P < 0$ , indicates an inward flow.

**Other Effects** Other factors also contribute to the pressure difference between the interior and exterior. Some examples of these are various combustion processes (fireplaces), ventilation fans, or even human factors such as opening and closing doors or windows.

### 1.3.4 Indoor Sources

There are two types of indoor sources in VI. The first are various products and items that contain the contaminant of concern and continuously emit these. Some examples of these may be various cleaning products, degreasers, gasoline tanks, or even recently dry-cleaned clothing. These are usually not considered to be part of the VI phenomena themselves (even though they can pose health risks) but rather items that need to be removed in a VI investigation to prevent false positives.

The second type are the walls, furniture, objects, or features inside the interior that sorb the contaminant vapors. While these are not *sources* in the strict sense, they may nevertheless contribute to the overall contaminant exposure. How significant these secondary types of indoor sources are largely depend on the material. Some, such as cinderblock concrete have a very large capacity to hold contaminant vapors while others such as fabrics do not.

**Sorption Processes** Modeling the secondary type indoor sources (sorption onto materials) can be done with a simple equilibrium reaction:

$$c^* \xrightleftharpoons[k_2]{k_1} c_{\text{in}} \quad (1.10)$$

## 1.4 Soil Physics Governing Vapor Intrusion

The soil surrounding the structure in our VI model is, unlike the indoor environment, modeled explicitly. In this section we will walk through each physics, the associated governing equation, and boundary conditions required to model the contaminant transport in soil. The following physics and governing equations will be covered:

1. Water flow in unsaturated porous media
2. Vapor transport in unsaturated porous media



### 3. Mass transport in partially saturated medium

In addition to these, the modeling of the temperature distribution in the soil is covered in Appendix .

The vapor contaminant transport through the soil in VI occurs through the vadose zone - soil that is partially filled with water, giving a three-phase transport system. This partial water content has profound effects on both advective and diffusive transport and modeling the water content is achieved via *Richard's equation*. Since the vapor and mass transport in the soil are so dependent on the soil water content, it is covered first in the following section 1.4.1.

The mass transport in the soil has both an advective and diffusive component. The advective transport in the soil is dictated by the vapor flow in the soil which is described by *Darcy's Law* making it the next logical step to cover in section 1.4.2. The diffusive transport depends on the contaminant vapor concentration itself and accurately modeling this requires coupling with all of the physics discussed so far (including the indoor environment). Therefore the mass transport physics, governed by the *advection-diffusion equation* will be covered last in section 1.4.3.

#### 1.4.1 Water Flow in Unsaturated Porous Media

The vadose zone or unsaturated zone is a region of soil between the top of the ground surface and the water table. In the vadose zone there are two fluid phases, one gas and the other liquid (usually air and water) inside the porous soil matrix giving a three phase system; only one fluid phase (gas or liquid) exist in the saturated zone. As a result, the transport properties in the vadose zone differ from that in a zone saturated where there are only two phases present - water and soil.

#### Soil-Water Potential and Retention Curve

The driving force, or soil-water potential, for the filling and draining of pore water in soils are due to a pressure and a gravitational potential and given by  $\phi$ . This phenomena is called *capillary potential* or *matrix potential*,  $\psi$ , which depends on the volumetric water content  $\theta$  in the soil.

Over the years, there has been a few attempts of characterizing the relationship between soil moisture content  $\theta$  and soil water potential  $\phi$  - a so-called soil water retention curve. Two common relationships have been proposed by Brooks and Corey in 1966[?], and another by van Genuchten in 1980[?]. Both of these approaches are semi-empirical and each is a function of the soil water potential with several fitting parameters. These parameters are specific to each soil type and usually are derived from laboratory experiments. In our VI models we chose to use the van Genuchten formulation for the simple reason that these have been historically used in VI modeling and the associated parameters are well-known for a variety of soils.

In the van Genuchten formulation that we use, pressure head  $H_p = \frac{p}{\rho g}$  is used as the dependent variable instead of the soil water potential  $\psi$ . Here  $p$  is the fluid pressure;  $\rho$  the fluid density; and  $g$  is the acceleration of gravity. The fluid is here water. By definition the soil matrix is saturated with fluid when the pressure head is zero  $H_p = 0$  and variably saturated for negative pressure heads,  $H_p < 0$ . The van

Genuchten equations express four properties:

$$\text{Se} = \begin{cases} \frac{1}{(1+|\alpha H_p|^n)^m} & H_p < 0 \\ 1 & H_p \geq 0 \end{cases} \quad (1.11)$$

$$\theta = \begin{cases} \theta_r + \text{Se}(\theta_s - \theta_r) & H_p < 0 \\ \theta_s & H_p \geq 0 \end{cases} \quad (1.12)$$

$$C_m = \begin{cases} \frac{\alpha m}{1-m}(\theta_s - \theta_r) \text{Se}^{\frac{1}{m}} (1 - \text{Se}^{\frac{1}{m}})^m & H_p < 0 \\ 0 & H_p \geq 0 \end{cases} \quad (1.13)$$

$$k_r = \begin{cases} \text{Se}^l [1 - (1 - \text{Se}^{\frac{1}{m}})]^2 & H_p < 0 \\ 0 & H_p \geq 0 \end{cases} \quad (1.14)$$

**Soil saturation** Se is the soil water saturation and ranges from 0 to 1, representing unsaturated and saturated respectively;  $H_p$  is the pressure head;  $\alpha$  and  $n$  are two van Genuchten parameters, with  $m = 1 - \frac{1}{n}$ .

**Soil moisture content**  $\theta$  is the volumetric soil moisture content or water-filled porosity;  $\theta_s$  is the saturated porosity, i.e. the total porosity of the soil matrix;  $\theta_r$  is the residual moisture content (even dry soils typically retain some moisture). The soil vapor or vapor-filled porosity is easily calculated by  $\theta_g = \theta_s - \theta$ .

**Specific moisture capacity**  $C_m$  is the specific moisture capacity which dictates the change in  $\theta$  with respect to changes in pressure  $p$ , i.e.  $\frac{\partial \theta}{\partial p}$ .

**Relative permeability**  $k_r$  is the relative permeability and just like Se ranges from 0 to, representing the soil matrix being fully impermeable and permeable to a particular fluid. The formulation in (1.14) is for water, but the vapor relative permeability is simple  $1 - k_r$ .

In Figure 1.4 the soil water retention curves for sandy loam soils are shown. Notice how the saturation is significantly higher slightly above the groundwater, this is called the capillary fringe and presents a significantly barrier to vapor transport, as we will see in future sections

Figure 1.4: Retention curves for sandy loam soil.

## Richard's Equation

The change in soil moisture through a soil domain is the sum of any change in flux of water in or out of the soil domain. In 1931 Lorenzo Richards[?] developed an eponymous PDE that describes this. Richards' equation itself is an extension of Darcy's Law, which governs fluid flow in saturated media (more on this in section 1.4.2).

$$\rho \left( \frac{C_m}{\rho g} + \text{Se} S \right) \frac{\partial p}{\partial t} + \nabla \cdot \rho \left( - \frac{\kappa_s}{\mu} k_r (\nabla p + \rho g \nabla D) \right) = Q_m \quad (1.15)$$

Here  $p$  is the capillary potential;  $C_m$  is the specific moisture capacity;  $S_e$  is the effective saturation;  $S$  is the storage coefficient;  $\kappa_s$  is the saturated permeability of the porous media;  $\mu$  is the fluid viscosity;  $k_r$  is the effective permeability;  $\rho$  is the fluid density;  $g$  is the acceleration of gravity;  $D$  is the elevation or head; and  $Q_m$  is a source term, a positive or negative value represent a source or sink respectively.

In the VI model that we are developing we usually assume that there is no change in soil moisture content w.r.t. time, i.e. that it is at steady-state, and that there is no source or sink present, greatly simplifying (1.15). Since we're solving the PDE at steady-state, it is not that important to specify any initial values (although it can reduce computation time), but we need to specify a few boundary conditions to solve (1.15).

**Boundary conditions** In the simplest case only three boundary conditions need to be specified. The first two are Dirichlet boundary conditions<sup>1</sup> where we specify the pressure to be zero at the water table boundary (bottom of the model) and at the ground surface the pressure head is equal the negative of the depth to the water table. The third is a no-flow boundary condition<sup>2</sup>, specifying that there is no soil moisture flux through these boundaries, is applied to all other boundaries.

$$p_{\text{water-table}} = 0 \text{ (Pa)} \quad (1.16)$$

$$p_{\text{ground-surface}} = -z_{\text{water-table}}\rho_{\text{water}}g \text{ (Pa)} \quad (1.17)$$

$$(\text{All other}) - \vec{n} \cdot \rho_{\text{water}}\vec{u} = 0 \quad (1.18)$$

Where  $\rho_{\text{water}}$  is the density of water;  $z_{\text{water-table}}$  is the depth of the water table relative to the ground surface;  $g$  is the acceleration of gravity;  $\vec{n}$  is the a boundary's normal vector;  $\vec{u}$  is the velocity vector of the water moving in the soil matrix.

## 1.4.2 Vapor Transport in Unsaturated Porous Media

Fluid transport in porous media is governed by *Darcy's Law* and was originally formulated by Henry Darcy based on his work on describing water flow through soil under the influence of gravity. Since then it been found to derivable in several ways from the Navier-Stokes equations[?] and may be stated as a pressure gradient driven velocity.

$$\vec{u} = -\frac{\kappa}{\mu}\nabla p \quad (1.19)$$

Here  $\vec{u}$  is the fluid velocity;  $\kappa$  the soil permeability;  $\mu$  is the fluid viscosity; and  $\nabla p$  is the pressure gradient. In VI modeling we're interested in the flow of contaminant vapors but since the contaminant concentrations are typically very low, the transport properties may be taken from those of pure air.

For Darcy's Law to be valid, two assumptions must be fulfilled:

1. The fluid must be in the laminar regime, typically  $Re < 1$ .
2. The soil matrix must be saturated with the fluid.

---

<sup>1</sup>A prescribed fixed value to the dependent value at the boundary.

<sup>2</sup>A Neumann boundary condition.

Typically the vapor flows in most VI scenarios are sufficiently slow for the first condition to be fulfilled. And if they are not, there are modifications to Darcy's Law that Most of the contaminant vapor transport takes place in the partially saturated vadose zone and thus, (1.19) needs modification.

In partially saturated soils, a varying portion of the soil pores are available for vapor transport, with the rest being occupied by water, affecting the effective permeability of the soil. To model this, a relative permeability property,  $k_r$ , is introduced:

$$\kappa_{\text{eff}} = k_r \kappa_s \quad (1.20)$$

$k_r$  is a dimensionless parameter that varies between 0 and 1, and  $\kappa_s$  is the saturated, or simply the soil matrix permeability.

This gives the modified Darcy's Law used in VI-modeling:

$$\vec{u} = -\frac{k_r \kappa_s}{\mu} \nabla p \quad (1.21)$$

### 1.4.3 Mass Transport in Unsaturated Porous Media

$$\frac{\partial}{\partial t}(\theta c_i) + \frac{\partial}{\partial t}(\rho_b c_{P,i}) + \frac{\partial}{\partial t}(a_v c_{G,i}) + \vec{u} \cdot \nabla c_i = \nabla \cdot [(D_{D,i} + D_{eff,i}) \nabla c_i] + R_i + S_i \quad (1.22)$$

## 1.5 Meshing

## 1.6 Solver Configuration

## 1.7 References